Stars and Nuclei: A Tribute to Manuel Forestini
T. Montmerle et C. Kahane (eds)
EAS Publications Series, Vol. 19 (2008) 103-124

EVOLUTION OF MASSIVE AGB STARS

Lionel Siess[1]

Abstract. The evolution of stars in the mass range 7-12$M_\odot$ is characterized by the off-center ignition of carbon in condition of partially degeneracy followed by the propagation of a convectively bound flame and the formation of a neon-oxygen core. In this chapter, we review the evolutionary features of these peculiar stars and pay a special attention to the thermally pulsing super-AGB phase and associated nucleosynthesis. The evolution toward electron capture supernovae for the most massive members of this class is briefly mentioned. In light of new computations, we also discuss the question of $M_{\rm up}$, the critical mass above which carbon ignites as well as $M_{\rm n}$, the minimum mass for the formation of a neutron star and analyze the dependence of these transition masses on metallicity.

1 Introduction

At the end of central helium burning, the core of low and intermediate mass stars ($M \lesssim 7-9M_\odot$) experiences efficient neutrino cooling and owing to its small mass, becomes strongly degenerate. The temperature maximum moves outward and nuclear burning then proceeds in a shell. Thereafter, the reactivation of the H burning shell (HBS) marks the beginning of the thermally pulsing AGB phase characterized by the development of recurrent instabilities in the He burning shell (HeBS). In this final stage of the evolution, the envelope is expelled by the strong winds powered by the high stellar luminosity and a planetary nebula forms. The star is now a CO white dwarf of typical mass $\sim 0.6M_\odot$, doomed to radiate aways its internal energy and crystallize. On the other hand, in massive stars ($M \gtrsim 12M_\odot$) the degenerate electron pressure cannot overcome the gravitational pull of the core. The central regions contract and despite increasing neutrino energy losses, the central temperature increases. Carbon then ignites at the center and the

L.S. is FNRS research associate

[1] Institut d'Astronomie et d'Astrophysique, Université Libre de Bruxelles, CP 226, B-1050 Brussels, Belgium

DOI: (will be inserted later)

evolution proceeds through all the nuclear burning stages (neon photo-dissociation, oxygen and silicon burning). Then, depending on the mass of the iron core, the supernovae explosion will give birth to a neutron star or a black hole.

In this short and incomplete sketch of stellar evolution, a class of star is missing : the ones that make the link between intermediate and massive stars. These objects, which mass ranges between $\sim 7-12M_{\odot}$ are the main topic of this chapter and will sometimes be abusively refereed to as "massive AGB stars".

The study of massive AGB stars dates back to the late 60's and early 70's with different works (Rakavy *et al.* 1967, Beaudet & Salpeter 1969, Boozer *et al.* 1973) analyzing the evolution of CO stars in the mass range $1.03-1.44M_{\odot}$. In these early studies, it was soon realized that carbon could ignite off-center at relatively low density ($\rho \lesssim 10^7\mathrm{g\,cm^{-3}}$). Then, Barkat *et al.* (1974) ran the first consistent computation of the evolution of a $8M_{\odot}$, from the main sequence to the formation of a SiO core. The authors also pointed out the possibility that stars of about this mass could be the progenitors of pulsars. The 80's focused on the advanced and hydrodynamic stages of the evolution of NeO cores. The pioneering works of Nomoto and collaborators (Miyaji *et al.* 1980, Nomoto 1984, 1987, Miyaji & Nomoto 1987, Hashimoto *et al.* 1993) reveal the fundamental role played by electron captures in triggering the collapse of the core. These studies were then followed by some rare hydrodynamical simulations (e.g. Hillebrandt *et al.* 1984, Baron *et al.* 1987, Mayle & Wilson 1988). More recently, the literature attests of a reviving interest in these stars (Garcia Berro *et al.* 1994, 1997, Iben *et al.* 1997, Ritossa *et al.* 1996, 1999, Bono *et al.* 2000, Eldridge & Tout 2004, Siess 2006) and this paper is another illustration.

In the following section, we briefly overview the evolution prior to carbon ignition which is very similar to that of a typical intermediate mass star. Then in Sect. 3, we describe the carbon burning phase, the flame propagation and the composition of the NeO core. The characteristics of the second dredge-up are described in Sect. 4 and in Sect. 5, we discuss the super-AGB (SAGB) phase and associated nucleosynthesis. The fate of the most massive members of this mass range is briefly sketched in Sect. 6 and before concluding, we introduce different mass transitions and analyze their dependence on metallicity.

2 Evolution prior to Carbon Ignition

Prior to carbon ignition, the evolution of the internal structure is very similar to that of standard intermediate mass stars (Fig. 1). During the main sequence, H burning takes place in a convective core and operates through the CNO cycle. When a pure He core is formed, H burning moves off-center in a shell. The core, deprived of nuclear energy sources, contracts while the envelope expands and deepens in the stellar interior. During the so-called first dredge-up, the surface convective zone penetrates into the regions affected by H burning and the surface composition changes. Similarly to lower mass stars, the hydrogen mass fraction decreases to the benefit of helium and the surface abundances exhibit the chemical signatures of the operation of the incomplete CN and ON1 cycles: ^{12}C and ^{16}O are

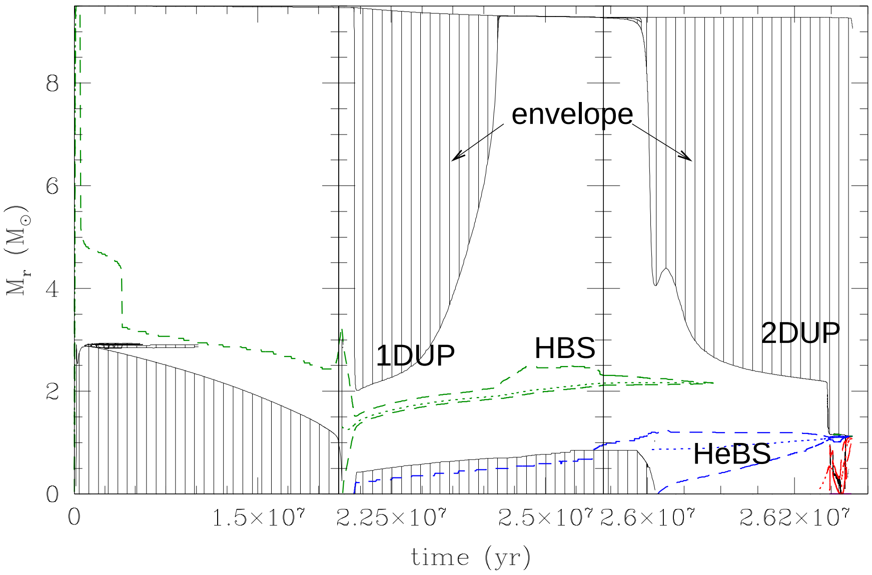

Fig. 1. Kippenhahn diagram of the evolution of a $9.5M_\odot$ up to carbon ignition. The dotted (green) and dashed (blue) lines indicate the location of the maximum nuclear energy production by H and He burning, respectively. Convective regions are represented by hatched areas.

depleted while ^{17}O, ^{13}C and ^{14}N are increased. The number ratios ^{12}C/^{13}C and ^{12}C/^{16}O both decrease to reach typical values of ~ 20 and ~ 0.32, respectively. The chemical signatures of the first dredge-up are the same in the $9-12M_\odot$ models as in lower mass stars so, as far as the chemical composition is concerned, they are almost indistinguishable from their lower mass counterparts.

When the central temperature reaches $\sim 10^8$K, He ignites and a convective core forms. The 3α reactions power the star until the core He mass fraction drops below ~ 0.1 where the ^{12}C$(\alpha,\gamma)^{16}$O reaction takes over the nuclear energy production. The activation of this latter reaction decreases the C/O ratio which final value remains highly dependent on the adopted reaction rate for ^{12}C(α,γ) and also on the efficiency (semi-convection, overshooting) and duration of convective mixing in the late stage of He-core burning (e.g. Straniero *et al.* 2003).

Nucleosynthesis during core He burning leads to the production of ^{12}C and ^{16}O and to the conversion of the ashes of H burning into ^{22}Ne and ^{16}O by α captures on ^{14}N and (α,n) reactions on ^{13}C, respectively. Because in massive AGB stars the temperature in the convective core remains relatively low ($T_{\rm c} \lesssim 3\times10^8$K), the ^{22}Ne($\alpha$,n)^{25}Mg reaction is not very efficient. The neutron density never exceeds $N_n \lesssim 10^5$cm^{-3} and the neutron exposure remains lower than ~ 0.015 mbar^{-1}. Therefore no s-process nucleosynthesis is expected to take place at this stage, contrarily to massive stars. We note however a slight production of ^{25}Mg, ^{26}Mg and ^{17}O as a result of neutron capture reactions.

3 The Carbon burning Phase

3.1 Global evolution

Following central helium exhaustion, core contraction resumes while the surface layers expand. In low and intermediate mass stars, electrons become degenerate. At the center, the heat lost by plasma neutrino exceeds the heat gain due to gravitational contraction and a temperature inversion appears. The maximum temperature moves off-center and increases in magnitude, but because of the small core mass, the threshold value for carbon ignition cannot be reached. The peak temperature passes through a maximum and then decreases as the increasing central density boosts the neutrino energy loss rate. On the other hand, massive stars do not develop degenerate cores and carbon ignites at the center.

The main specificity of the presently studied stars comes from the fact that the off-center peak temperature reaches $\sim 7 \times 10^8$K and that carbon ignites. The evolution during the carbon burning phase is very similar among stars of this class and our analyze will be based on a representative $9.5 M_\odot$ model (Fig. 2). In all cases, carbon burning proceeds in two stages. First, the development of a violent carbon flash which induces the quenching of the instability and the return of core contraction and then a "softer" carbon re-ignition and the development of a flame that propagates to the center (Ritossa *et al.* 1996, Siess 2006).

When carbon ignites, because of the partial degeneracy ($\eta \sim 2-3$) there is a delay between the start of energy deposition and the structural response of the star. At the ignition point, heat accumulates, the nuclear energy production increases and a thermal runaway develops leading to a carbon flash. In this region, the temperature gradient becomes steeper and convection sets in. As the instability grows, the energy released by carbon burning is mostly converted into mechanical work and a large expansion of the structure ensues which also affects the core as can be seen in Fig. 3 from the decrease in both the central temperature (T_c) and density (ρ_c). The structural response of the star to carbon ignition provokes the quenching of the instability, the return to core contraction and the disappearance of convection. Note that part of the energy absorbed by the core during the flash was used to lift the degeneracy. As a consequence, the peak temperature has moved deeper and when it reaches again the critical value for carbon ignition a new instability develops. The ignition conditions are however much different than during the flash. First, the degeneracy is lower ($\eta \sim 1$ compared to $2-3$) so the instability is weaker (the carbon luminosity $L_C \simeq 1.2 \times 10^6 L_\odot$ compared to $1.5 \times 10^7 L_\odot$ during the flash) and second, the convective zone develops in the regions that were previously occupied by the flash. As a consequence less fuel is available[1] and the release of nuclear energy is thus reduced. In these conditions,

[1]For carbon burning, the nuclear energy production rate is proportional to the square of the

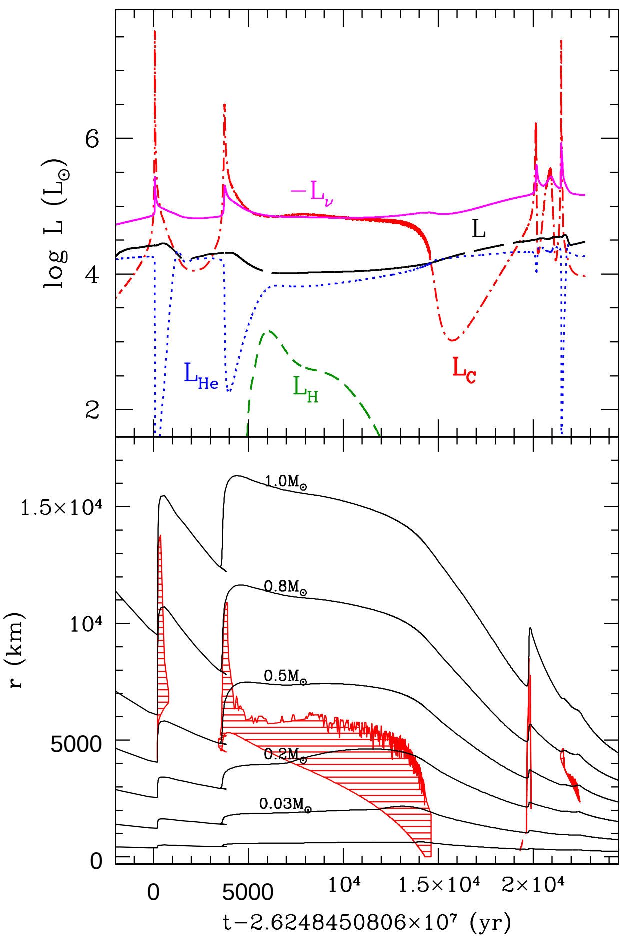

Fig. 2. Structural and energetic evolution of a $9.5M_\odot$, solar metallicity model during the carbon burning phase. In the upper panel, the nuclear luminosities associated with H (L_H), He (L_He) and C (L_C) burning are shown as well as the neutrino (L_ν) and surface (L) luminosities. In the eulerian view of the Kippenhahn diagram (bottom panel), the solid lines correspond to isomass contours equal to 0.001, 0.03, 0.2, 0.5, 0.8 and 1.0 $M_\odot$. Convective regions are represented by hatched areas.

the instability, which becomes a flame, is not quenched because the expansion of the structure is moderate. This "soft" ignition allows a steady state to be achieved where most of the energy deposited at the base of the flame can be evacuated in the convective zone by the neutrinos (Timmes *et al.* 1994). In the radiative layers located at the base of the convective flame, the nuclear energy production is maximum. In this so-called "precursor flame" (Garcia-Berro *et al.* 1997), material is heated and the temperature profile becomes steeper. The transport of energy changes, the shell becomes convective and the flame moves inward, engulfing at the same time the ashes of carbon burning.

After a period spanning a few thousand years, the flame reaches the center and convection disappears. Carbon burning then proceeds radiatively in a shell

carbon abundance.

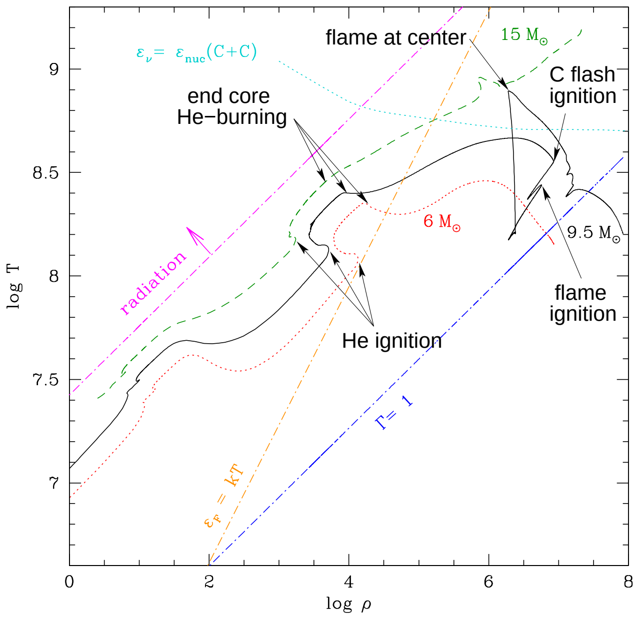

Fig. 3. Evolution of a 6 (dotted), 9.5 (solid) and $15 M_{\odot}$ (dashed) stars in the $\rho_c - T_c$ plane. The lines delineating degeneracy (Fermi energy = thermal energy) and non-ideal effects ($\Gamma = 1$) are also shown as well as the locus where the neutrino emission rate (ε_{ν}) equal the nuclear energy production by $^{12}C+^{12}C$ reactions ($\varepsilon_{\rm nuc}$).

surrounding the NeO core. When this burning shell meets some carbon pockets left at the edge of the core, secondary convection zone form (Fig. 4).

3.2 Evolution at $Z = Z_{\odot}$ as a function of initial mass

Our models at solar metallicity, which do not include extra mixing beyond the Schwarzschild limit, indicate that off-center carbon ignition is restricted to a very narrow mass range between 9 and $11.3 M_{\odot}$. As the initial mass increases, carbon ignition occurs closer to the center and the strength of the flash decreases. This is a direct consequence of the decreasing core degeneracy as the mass increases. In the limit of no degeneracy, carbon ignites quietly at the center as in massive stars.

The duration of the carbon flash varies between ~ 200 yr and 6800 yr, depending on the stellar mass (Siess 2006). Schematically, its value depends on two main factors namely the carbon content in the convective flash which in turn depends on the extent of the convective flash and on the rate at which it is depleted which are function of the thermodynamical conditions in the flash. The duration of the flash is thus governed by the competing effects of fuel replenishment by growing convection and fuel depletion and is maximum around $10.5 M_{\odot}$.

As the mass increases, the flame ignites closer to the center and therefore reaches the center more rapidly. The duration varies between 600 yr and $\sim$ 13500 yr for a 10.8 and $9 M_{\odot}$ model, respectively. Note also that in more massive stars, the temperature in the flame front is higher and the deflagration velocity which scales as $\sqrt{\rho}T^{14}$ (Timmes *et al.* 1994), is larger. Typical values of the flame speed ranges between 1.5×10^{-3} and 2.2×10^{-2}cm s^{-1}.

Finally, let us mention that if the flash ignites very close to the center (as for the $11.3M_\odot$ models where carbon ignites at a mass coordinate of $0.015M_\odot$), there is no flame. The convective zone associated with the flash reaches directly the center and then carbon burning proceeds in a convective core, as in massive stars.

3.3 Carbon nucleosynthesis and the composition of the neon-oxygen core

Carbon burning proceeds through ^{12}C(^{12}C,α)^{20}Ne and ^{12}C(^{12}C,p)^{23}Na reactions followed in third place by ^{16}O(α,γ)^{20}Ne. These reactions convert the CO core into a NeO mixture and supply protons and α particles for a richer nucleosynthesis.

When carbon ignites, the composition of the core is principally made of ^{16}O ($\sim 0.63-0.73$)[2], ^{12}C ($\sim 0.34-0.24$) with some remaining ^{22}Ne ($\lesssim 2\%$) produced earlier during the core He burning phase on the ashes of hydrogen burning (^{14}N mainly).

In the carbon burning zone, the α particles that are not captured by ^{16}O react with ^{22}Ne and produce the heavy Mg isotopes plus some neutrons via the (α,n) channel. These neutrons are then captured by the abundant ^{16}O and to a lower extent by ^{20}Ne, ^{23}Na and ^{25}Mg, leading the production of ^{17}O, ^{21}Ne, ^{24}Mg and ^{26}Mg. The protons released by ^{12}C(^{12}C,p)^{23}Na contribute to the production of ^{20}Ne and ^{24}Mg by (p,α) and (p,γ) reactions on ^{23}Na, and to the synthesis of ^{27}Al by (p,γ) reactions on ^{26}Mg. The incineration of the core after the passage of the flame leads to a compact structure composed mainly of ^{16}O ($\sim 55-60\%$), ^{20}Ne ($\sim 28-32\%$), ^{23}Na ($\sim 5.5\%$), ^{24}Mg ($\sim 3.3\%$) and ^{25}Mg ($\sim 1.5\%$).

4 The second dredge-up phase

Following central He exhaustion, the gravothermal energy released by core contraction is converted into heating, leading eventually to carbon ignition, and into mechanical work used to expand the outer layers. In the radiative shells below the convective envelope where most of the energy is deposited, the density and temperature decrease causing an increase in the opacity coefficient (κ) and concomitantly of the radiative gradient $\nabla_{\rm rad}$ ($\propto \kappa T^{-4}$) which becomes larger than its adiabatic value $\nabla_{\rm ad}$. The convective envelope deepens in the so-called second dredge up (2DUP) phenomenon. However, depending on the initial stellar mass, the completion of the 2DUP takes place before, during or at the end of carbon burning (see Garcia-Berro *et al.* 1997 for a detailed analysis). In stars of lower mass, e.g. in the 9 and $9.5M_\odot$ models, the 2DUP has enough time to reach completion before carbon ignites. However, in our $10.8M_\odot$ model the evolution is slightly different : after central carbon exhaustion, a convective zone develops in the HeBS, grows in mass and merges with the envelope (Fig. 4). This so-called

[2]the range of values correspond to the various compositions found in solar metallicity models covering the mass range $9-12M_\odot$.

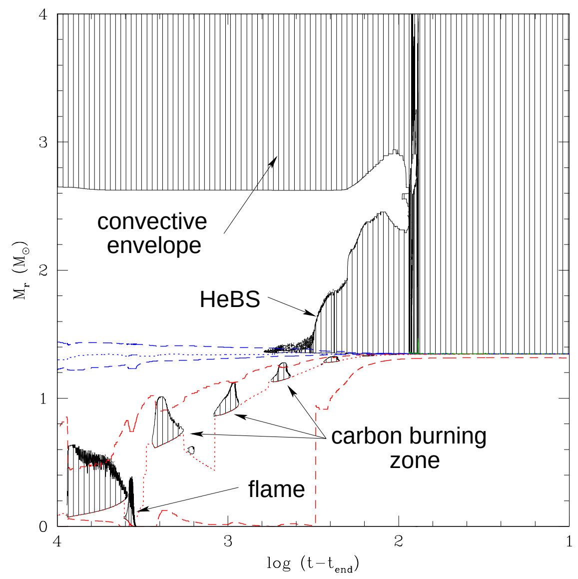

Fig. 4. Dredge-out phenomenon at the end of carbon burning during which the convective zone that develops in the HeBS merges with the envelope. This process, shown here in a $10.8M_\odot$ of initial solar composition, contributes to decrease the mass of the He-exhausted core and to pollute further the envelope.

dredge-out process (Iben *et al.* 1997) increases the depth of the 2DUP and has important consequences since it decreases substantially (by $\gtrsim 1M_\odot$) the size of the H-exhausted core (see § 7.4).

During the 2DUP, the envelope crosses the HBS and enriches the surface with ^{14}N mostly to the expense of ^{12}C, ^{13}C, ^{15}N, ^{16}O and ^{17}O. However, in stars that experience the 2DUP during the carbon burning phase or a "dredge-out" process, the envelope reaches the HeBS. This increases the surface abundance of ^{4}He mainly, but also of ^{18}O, ^{22}Ne and restore part of the ^{12}C.

5 The super-AGB phase

The fate of stars in this transition region is very dependent on the mass loss rate and internal mixing processes which are unfortunately largely unknown. In the early 80's, thanks to the works of Nomoto and collaborators, it has been realized that if the NeO core mass reaches or exceeds a critical value of $M_{\rm EC} \sim 1.37M_\odot$, then the core would collapse and produce a supernovae explosion (see §6). Whether or not the stellar mass can reach $M_{\rm EC}$ then depends on the competition between core growth and mass loss. In this section, we consider the evolution of stars for which the core mass remains less than $M_{\rm EC}$.

5.1 Early-AGB phase

At the end of carbon burning, as the density and degeneracy increase in the core, the contraction rate of the central regions slows down. The gravothermal heat source fades and, as neutrino losses increase, carbon burning quenches. The stellar energy production is then supplied almost entirely by the HeBS since H burning has been switched-off during the 2DUP. During the so called “early-AGB phase”, the convective envelope retreats and the HeBS progresses in mass until it approaches the H-He discontinuity. There, it losses its efficiency and allows the overlying layers to contract and re-heat. The HBS then reignites and the star enters the thermally pulsing SAGB (TP-SAGB) phase.

5.2 Thermally pulsing super-AGB phase

As in lower mass stars, recurrent thermal instabilities develop in the HeBS of SAGB stars. Their origin comes from the conjunction of 3 factors (Schwarzschild & Harm 1965) : the 3α reaction rate is very temperature sensitive, the region of nuclear energy production is geometrically thin and the HeBS is optically thick. All these conditions lead to the deposition of energy at the ignition point. Because of the geometrical confinement of the burning region, the gravity of the shell remains almost constant and assuming hydrostatic equilibrium, the equation of motion imposes that the pressure remains also constant. Therefore, the heat deposition does not necessarily lead to a structural readjustment. Provided the shell is optically thick so that the excess thermal energy cannot escape too easily, the temperature rises, the nuclear reaction rate increases releasing more heat and a thermonuclear runaway ensues.

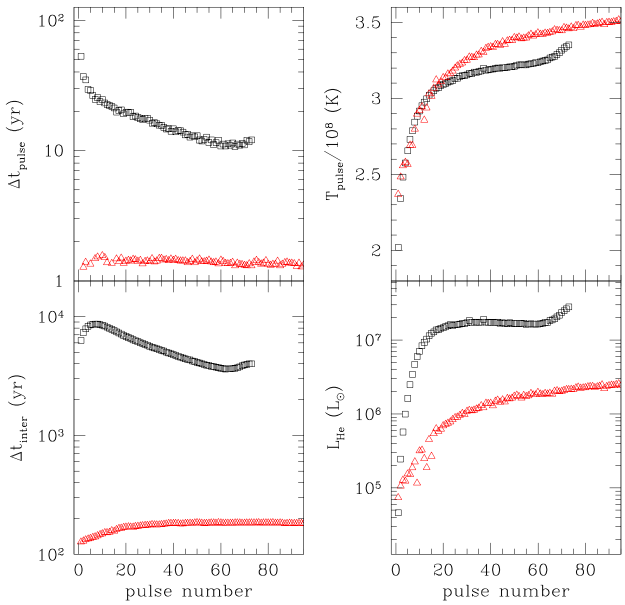

Fig. 5. Selected properties of the TP-AGB evolution of a $5M_\odot$ (square) and $10M_\odot$ (triangle) as a function of pulse number. The interpulse ($\Delta t_{\rm inter}$), pulse duration ($\Delta t_{\rm pulse}$) and maximum He luminosity ($L_{\rm He}$) are a decreasing function of the stellar mass while the temperature at the base of the pulse ($T_{\rm pulse}$) increases with $M_{\rm c}$.

During the interpulse period, the star’s luminosity is mostly provided by the HBS (> 80%). Helium burning is almost switched-off and the ashes of H burn-

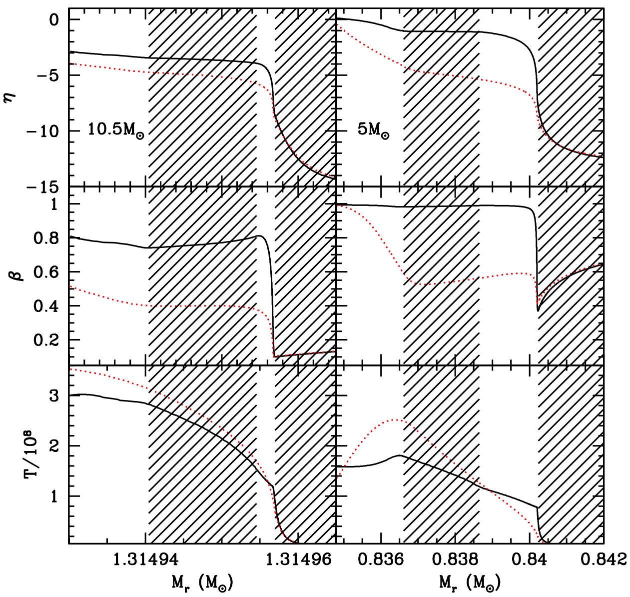

Fig. 6. Profiles of temperature (T), ratio of gas pressure to total pressure (β) and degeneracy parameter (η) inside the HeBS of a $10.5M_\odot$ (left panel) and $5M_\odot$ (right panel). The solid and dotted lines correspond to profiles taken at the beginning and just after extinction of the pulse, respectively. The hatched areas represent the convective regions (pulse and envelope).

ing progressively increase the mass of the He buffer. In the growing HeBS, the temperature increases and when a critical mass has been accreted, He ignites in conditions of partial degeneracy. In the mechanism previously introduced, a convective instability develops, the thermal pulse, that engulfs all the material previously processed by the HBS. As we will examine later, the combination of this chemical mixing with the high temperatures achieved in the pulse gives rise to a rich nucleosynthesis.

The evolution during the AGB phase is primarily governed by the core mass M_c. Qualitatively, as M_c increases, the interpulse and pulse durations shorten. Put into numbers this leads, for solar metallicity models, to an interpulse duration of $\sim$ 4000 yr in a $5M_\odot$ models (with $M_\mathrm{c} = 0.9M_\odot$) compared to 180 yr in a $10M_\odot$ ($M_\mathrm{c} = 1.2M_\odot$) and $\lesssim 30$ yr in a $10.5M_\odot$ models ($M_\mathrm{c} = 1.31M_\odot$). For the same stars, the convective instability lasts $\sim$ 15, 1.5 and 0.4 yr for the 5, 10 and $10.5M_\odot$ models, respectively. Considering the large envelope mass of SAGB stars ($\sim 8 - 10M_\odot$), the short interpulse duration (a few hundred years) and assuming an average mass loss rate of $\sim 10^{-4}M_\odot$, one may expect between 500 and $\sim$ 1000 thermal pulses before the total ejection of the envelope, a number much larger than in standard AGB stars !

Selected pulse characteristics are displayed in Fig. 5. In particular we note that, as M_c increases, the temperature and density at the base of the pulse increase while the extent of the convective instability decreases. This can be explained by the fact that when M_c is large, the HeBS is more compressed and therefore thinner and hotter. The strength of the pulse, as measured by the nuclear luminosity in the HeBS (L_He) is also weaker in our SAGB models. To understand the origin of this behavior, we note (Fig. 6) that in the pulse region the degeneracy parameter (η) and the ratio of gas pressure to total pressure (β) are smaller in SAGB compared to AGB stars. These conditions (higher radiation pressure, lower degeneracy and higher temperature) contribute to make the thermal instability weaker in SAGB stars (Yoon *et al.* 2004). Indeed at lower degeneracy, the pressure responds more rapidly to a temperature perturbation so less heat accumulates, at higher temperatures, the dependence of the nuclear reaction rate on temperature decreases so the runaway is slower and finally the substantial contribution of radiation pressure to the total pressure also implies that a small temperature excess will induce a substantial expansion ($P_{\rm rad} \propto T^4$). Although the HeBS is thinner in SAGB stars, it is also located at a smaller radius owing to their higher central density so the relative shell thickness (the parameter α_s in Yoon *et al.* 2004) remains very similar in a 5 and $10.5 M_\odot$ stars. The maximum luminosity in the He shell hardly reaches a few $10^6 L_\odot$ in our SAGB models while it rapidly exceeds $10^7 L_\odot$ in the $5 M_\odot$ star.

Because of the relative weakness of the helium shell flash, the HBS remains active during the entire pulse period while it is extinct in the $5 M_\odot$. Another property of SAGB stars is the much higher temperature found at the base of the convective envelope which reaches 8×10^7K in the $10.5 M_\odot$ compared with at most 2×10^7K in the $5 M_\odot$ model. As we will see in the next section, the maintenance of H burning at the base of the envelope has important consequences on the evolution and nucleosynthesis.

5.3 The third dredge-up

The third dredge-up (3DUP) corresponds to the penetration of the convective envelope in the region previously occupied by the thermal pulse after the latter deactivates. This mixing event is not easy to trigger because the envelope (composed mainly of H and He) must cross a large barrier of mean molecular weight to reach the C-rich layers left by the pulse and also because it costs energy to lift the heavier elements of the HeBS into the envelope. This process is also hampered by the presence of an active HBS. In addition, the 3DUP appears to be very dependent on the presence or not of mixing processes at the base of the envelope (e.g. Mowlavi 1999, Herwig 2000) but also on the numerics (Straniero *et al.* 1997, Pols & Tout 2001), on the definition of the convective boundaries (Frost & Lattanzio 1996), on the mixing length parameter (Boothroyd & Sackmann 1988) or on hypothesis concerning the entropy of mixing (Wood 1981). As a general rule, the stronger the thermal pulse and the lower the metallicity, the easier it is to trigger the 3DUP. At lower metallicity, the entropy barrier between the envelope and the pulse region is smaller and these conditions facilitate the penetration of convective envelope.

Our solar metallicity models, which do not include extra-mixing, are unable to develop 3DUPs. This is not surprising considering the relative weakness of the thermal pulse and the persistence of H burning. However in some test models where overshooting was included, we find that the 3DUP develops after 7 thermal pulses.

The 3DUP brings to the surface the products synthesized in the pulse. It is responsible for the formation of carbon stars[3] and for the detection of a large number of species including ^{19}F, the Mg and Al isotopes or the s-elements. Note that SAGB stars are characterized by a massive envelope and small pulses ; their mass extent is at least factor of 10 smaller than in standard AGB stars ($\sim 10^{-4}M_\odot$ in a $10M_\odot$ compared to a few $10^{-3}M_\odot$ in a $5M_\odot$). In these circumstances, the dilution factors are much larger in SAGB stars than in standard AGB stars. Therefore, to obtain an equivalent surface enrichment, SAGB stars need to undergo many more 3DUPs.

5.4 Nucleosynthesis

5.4.1 Pulse nucleosynthesis

SAGB stars represent a unique site in stellar evolution where the products of hydrogen burning (mainly ^{14}N, ^{13}C and ^{15}N) can reach the high temperatures at the base of the HeBS during the thermal pulse. In these conditions, ^{13}C is destroyed by (α,n) reactions and releases neutrons rapidly absorbed by the iron peak elements and by ^{14}N. This latter element also enters the chain of reaction $^{14}\mathrm{N}(\alpha,\gamma)^{18}\mathrm{O}(\alpha,\gamma)^{22}\mathrm{Ne}$ and leads to the production of ^{18}O and ^{22}Ne. The other isotope of nitrogen, ^{15}N, is mainly depleted by $^{15}\mathrm{N}(\alpha,\gamma)^{19}\mathrm{F}$ reactions. Fluorine production is particularly interesting because it is a good tracer of the nucleosynthesis operating in the pulse and also because its observation provides strong constraints on the models. The synthesis of ^{19}F is rather complex and follows the chain of reactions $^{14}\mathrm{N}(\alpha,\gamma)^{18}\mathrm{F}(\beta^+)^{18}\mathrm{O}(\mathrm{p},\alpha)^{15}\mathrm{N}(\alpha,\gamma)^{19}\mathrm{F}$ where the protons are provided by (n,p) reactions on ^{14}N. However, if the temperature in the pulse is too high ($T \gtrsim 2.8 \times 10^8$K), fluorine is destroyed by $^{19}\mathrm{F}(\alpha,\mathrm{p})^{22}\mathrm{Ne}$. Finally, if the temperature at the base of the pulse exceeds $\sim 3.3 \times 10^8$K, as found in SAGB stars, a strong source of neutrons can be activated by $^{22}\mathrm{Ne}(\alpha,\mathrm{n})^{25}\mathrm{Mg}$ reactions (see §5.4.3).

5.4.2 Hot Bottom Burning

In massive and/or metal poor AGB stars, the temperature at the base of the convective envelope ($T_{\rm env}$) is high enough ($\gtrsim 3 \times 10^7$K) for H burning. This phenomenon is refereed to as Hot Bottom Burning (HBB) and leads to the production of ^{7}Li through the Cameron and Fowler (1971) mechanism. In this scenario, ^{7}Be is produced at the base of the envelope by the pp cycle, then convectively transported in the outer and cooler regions where is decays into ^{7}Li. However, the production of this element stops when the ^{3}He supply runs out and it is thereafter destroyed by proton captures. When $T_{\rm env} \gtrsim 5 \times 10^7$K, the CNO cycle comes into play at the base of the envelope and converts ^{12}C into ^{14}N and ^{13}C mainly. In such stars, the ^{12}C/^{16}O and ^{12}C/^{13}C ratios decrease substantially. Provided $T_{\rm env} \gtrsim 6 \times 10^7$K,

[3] a carbon star is defined by a surface C/O ratio larger than 1

HBB can also activate the NeNa and MgAl chains which contribute to the production of ^{23}Na, ^{26}Al and ^{27}Al mainly. But at these temperatures ^{19}F is destroyed by (p,α) reactions. Finally, let us note that if the temperature exceeds $T_{\rm env} \gtrsim 10^8$K, then ^{23}Na is destroyed to the benefit of ^{20}Ne and ^{24}Mg (e.g. Siess *et al.* 2002).

5.4.3 The s-process

S-elements are heavy nuclei located on the valley of stability in the nuclide chart. Their nucleosynthesis results from the slow capture of neutrons (by slow we mean neutron exposures less than 0.02 mbar^{-1}) followed by disintegrations on heavier nuclei, starting from the iron peak elements and stopping at ^{209}Bi. The production of these elements in AGB stars is provided by two main sources : ^{13}C(α,n)^{16}O and ^{22}Ne(α,n)^{25}Mg.

The first reaction operates at relatively low temperatures ($\gtrsim 9 \times 10^7$K) but requires that ^{13}C is initially produced. The formation of the so-called "^{13}C pocket" is still a major problem. Indeed, the mass of ^{13}C produced by the HBS and engulfed in the pulse is too small to account for the observed abundances of s-elements. Iben and Renzini (1982) first suggested that the ^{13}C pocket could be produced during the 3DUP by protons diffusion below the convective envelope in the C-rich layers left by the pulse. In this scenario, ^{13}C is synthesized by ^{12}C(p,γ)^{13}N(β^+)^{13}C and its radiative burning during the interpulse leads to the production of s-elements. However the mechanism at the origin of the mixing during the 3DUP remains largely unknown. Different scenarios have been investigated, considering diffusive overshooting (Goriely & Mowlavi 2000), rotationally induced mixing (Langer *et al.* 1999, Herwig *et al.* 2003, Siess *et al.* 2004) or gravity waves mixing (Denissenkov and Tout 2003). Parametric models defining arbitrarily the mass of the ^{13}C pocket (Gallino *et al.* 1998, Busso *et al.* 2001) were also able to account for observed distribution of s-elements but the process by which this pocket forms is unknown. The current model for rotational mixing does not seem to work very well because when the ^{13}C pocket is formed, it is subsequently polluted by ^{14}N which acts as a poison, absorbing most of the neutrons and thus decreasing dramatically the efficiency of the s-process. However, in this theory the effects of magnetic fields are not considered and may represent a severe limitation to this models (Siess *et al.* 2004 for details).

The gravity wave model, although very simplistic in its present formulation, represents an interesting and promising mechanism for the production of s-elements and clearly deserves additional investigations.

So far, the overshoot model is the most studied mechanism. Its successes lay on its predicted power and on comparisons with observations. For instance, this model was able to account for the increased production of heavy s-elements and in particular of lead in very metal deficient stars (e.g. Van Eck *et al.* 2001). An interesting aspect of this scenario arises when the temperature at the base of the convective envelope becomes relatively large ($T_{\rm env} \gtrsim 7 \times 10^7$K). In these conditions, typical of SAGB stars, nuclear burning and chemical transport operate on similar timescales meaning that protons burn while being transported. It results that the ^{13}C and ^{14}N profiles that build up, overlap and as for the rotationally induced mixing, the presence of ^{14}N inside the ^{13}C pocket inhibits the s-process nucleosynthesis (Goriely & Siess 2004).

The other neutron source ^{22}Ne(α,n)^{25}Mg is activated at the base of hot thermal pulse ($T \gtrsim 3.3 \times 10^8$K). The so called convective s-process is characterized by high neutron densities ($N_n \gtrsim 10^{11} - 10^{14}$cm^3) and is very short lived (a few years). It affects the branchings near ^{86}Kr, ^{87}Rb, ^{96}Zr or ^{115}Sn and also contributes to produce more light s-elements (Sr, Y, Zr) with respect to the heavy ones (Ba, La, Ce).

In view of these scenarios, the most promising site for the production of s-elements in SAGB stars is supposedly the convective s-process. The temperatures in the pulse are high enough to activate the ^{22}Ne(α,n) source and provided the 3DUP is present, then a potential envelope enrichment in s-elements can take place. However, as explained before, the elemental distribution of s-nuclei will certainly differ from that of standard AGB stars because a different neutron source is involved. Concerning mixing at the base of the convective envelope, at first sight this mechanism will not be the main source of s-elements because of the efficient HBB. However, this extra-mixing will contribute to increase the amount of ^{14}N that can be engulfed in the pulse. Consequently more ^{22}Ne can be synthesized by successive α captures on ^{14}N and additional neutrons are made available for the s-process (Goriely & Siess 2005). This interesting aspect of the nucleosynthesis in hot-AGB requires additional studies and may represent a promising mechanism for the production of s-elements in SAGB stars.

To summarize the complex nucleosynthesis taking place in AGB stars, we refer to the nice illustration designed by Manuel Forestini and reproduced in Fig. 7.

6 The supernovae explosion

The first investigations of the ultimate fate of massive SAGB stars (Miyaji *et al.* 1980, Nomoto 1984, 1987) showed that, if the NeO core mass exceeds $M_{\rm EC} \sim 1.37 M_\odot$ at the end of carbon burning, off-center Ne flashes occurs and the evolution then proceeds through the O-burning and Si-burning stages just as more massive stars do. The initial mass for stars using this path was estimated to range between $10 M_\odot \lesssim M \lesssim 12 M_\odot$ (Nomoto 1884). Note that above $\sim 12 M_\odot$, stars do not develop degenerate cores after C burning and Ne ignites at the center. On the other hand, lower mass stars will not ignite Ne just after C burning. They will enter the SAGB phase and develop strongly degenerate core that will grow in mass due to shell accretion. However, before Ne ignition becomes unavoidable when the mass approaches $M_{\rm EC}$, the electron Fermi energies at the center are already larger than the threshold for electron captures. So electron capture reactions start, first on ^{24}Mg and ^{24}Na and then on ^{20}Ne and ^{20}F. The resulting decrease in the electron number density (Y_e) has important consequences : (1) it reduces the electron pressure so the core starts contracting (initially quasi-hydrostatically), (2) the Chandrasekhar mass (which is proportional to Y_e^2) decreases so the collapse is accelerated and (3) the heating (by γ-ray emission) can ignite Ne and O burn-

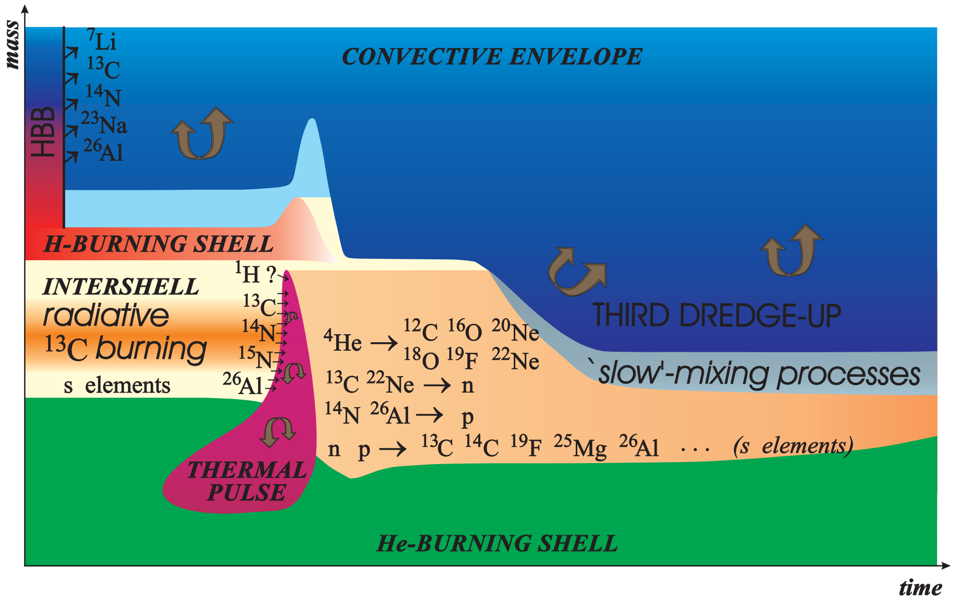

Fig. 7. Summary of the different sites and nuclear species involved in the nucleosynthesis of AGB stars, after Manuel Forestini.

ing. It also modifies the temperature gradient and may induce semiconvective or convective mixing. If these mixing processes come into play, then the complex physics of the convective URCA process must be taken into account. The increase of the core temperature leads to the central explosive ignition of Ne and O at densities $\rho_c \gtrsim 2 \times 10^{10}\,\mathrm{g\,cm^{-3}}$ (e.g. Miyaji & Nomoto 1987). Thereafter, the deflagration front that moves outward transforms the material to nuclear statistical equilibrium composition and fast electron captures on this material induces the final gravitational collapse (e.g. Gutierrez *et al.* 1996). Eventually nuclear densities are reached and a bounce shock forms supposedly able to remove the envelope (Hillebrandt *et al.* 1984).

This mechanism is refereed to as electron capture core collapse supernovae and is supposed to be at the origin of the formation of low-mass neutron stars (Fryer 1999). All these evolutionary aspects remain poorly studied and still affected by large uncertainties. The nucleosynthetic outcomes of these types of explosion are also highly speculative. It has notably been suggested that the propagation of the shock wave in the NeO rich layers during the hydrodynamical collapse may lead to a large production of neutrons by ^{22}Ne(α,n) and to the production of $r-$elements (Wheeler *et al.* 1998, Wanajo *et al.* 2003).

7 Mass transitions

Depending on the initial conditions and assumptions on the stellar mass, composition and mass loss rate, stars between 7 and $12 M_\odot$ can end their life in many different ways. They can either leave a CO white dwarf, a NeO white dwarf, or a neutron star as the result of electron capture or iron core collapse supernovae. The mass limit for stars that ignite carbon is traditionally refereed to as $M_{\rm up}$. We define $M_{\rm n}$ as the minimum initial mass for the formation of neutron stars and $M_{\rm SN}$ as the initial mass above which the evolution proceeds through all the nuclear burning stages and leads to a type II supernova. $M_{\rm SN}$ also corresponds to stars that develop (almost) non-degenerate NeO cores. These critical masses represent fundamental quantities which are related to many fields of astrophysics. For illustration, they allow to assess the supernovae and pulsar formation rates, to better understand the mass distribution of white dwarfs, the properties of novae or of planetary nebulae. They also have a direct impact on the chemical evolution of the Galaxy since, depending of the values of $M_{\rm up}$, $M_{\rm n}$ and $M_{\rm SN}$, different endings and nucleosynthesis outputs are expected.

Our study of the dependence of these transition masses on metallicity (Z) is based on the computation of a large grid of 74 stellar models (Siess & Pumo 2006) covering the initial mass ($M_{\rm ini}$) and metallicity range $7 M_\odot \leq M_{\rm ini} \leq 13 M_\odot$ and $10^{-5} \leq Z \leq 0.04$, respectively. The models were computed with the stellar evolution code STAREVOL (Siess 2006) initially developed by Manuel Forestini. We do not include extra-mixing such as overshooting and for the mass loss rate, we use the Reimers law prior to the SAGB phase with a metallicity dependence scaling as $(Z/Z_\odot)^{1/2}$ and then switch to the Vassiliadis and Wood (1993) prescription without metallicity dependence. When varying Z, the hydrogen and helium mass fractions are given by $X = X_{\rm BB} + (X_\odot - X_{\rm BB}) Z/Z_\odot$ and $Y = 1 - X - Z$, where the solar and primordial values equal $X_\odot = 0.710847$ and $X_{\rm BB} = 0.7521$ (Coc *et al.* 2004), respectively. The mass fraction of metals is scaled from the solar values of Grevesse *et al.* (1996).

7.1 A word of caution

Carbon ignition is primarily governed by the size of the CO core which in turn depends strongly on the mixing processes acting at the edge of the convective He core. The establishment of semiconvective regions in the outskirt of the convective core makes this boundary very sensitive to any perturbations and subject to important variations if some mixing processes associated with overshooting, rotation or gravity waves are included. The presence in some computations of breathing pulses is an illustration of the difficulty to model this phase and since our models do not include such mixing mechanisms, our values for the mass transitions should be considered as upper limits.

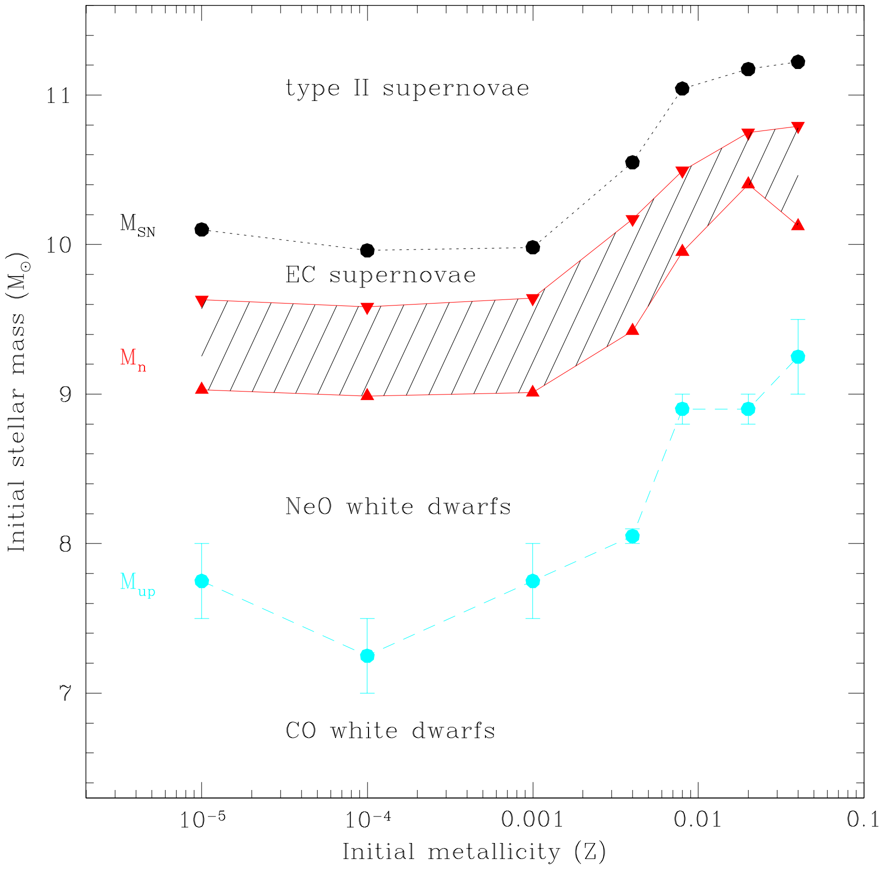

Fig. 8. Mass transitions as a function of metallicity Z. $M_{\rm up}$, $M_{\rm n}$ and $M_{\rm SN}$ correspond to the minimum initial stellar mass for carbon ignition, for the formation of a neutron star and for stars that will undergo type II supernovae, respectively. The shaded area represents the range of initial mass that will lead to neutron star formation when the mass loss rate is set to a constant value of $3 \times 10^{-5} M_\odot$ yr^{-1} (up triangle) and $10^{-4} M_\odot$ yr^{-1} (down triangle). The error bars for $M_{\rm up}$ correspond to our mass grid resolution. For instance, at $Z = 10^{-3}$, our $8M_\odot$ model ignites carbon while the $7.5M_\odot$ does not. This diagram also indicates the nature the stellar remnant : a CO white dwarf if $M_{\rm ini} < M_{\rm up}$, a NeO white dwarf if $M_{\rm up} \le M \le M_{\rm n}$ and above $M_{\rm n}$ it is a neutron star. Note the large uncertainty surrounding the estimate of $M_{\rm n}$.

7.2 $M_{\rm up}$: mass transition between CO and NeO white dwarfs

The dependence of $M_{\rm up}$ on the metallicity Z is shown in Fig. 8. Owing to their lower opacity, metal poor stars are more luminous and consequently develop hotter and more massive He cores. Therefore, when the metallicity decreases, the value of $M_{\rm up}$ decreases. At very low metallicity, typically below $Z \lesssim 10^{-4}$, we note however a reverse trend : $M_{\rm up}$ starts to increase with decreasing Z. As explained in Cassisi and Castellani (1993), this results from the fact that at very low metallicity the contribution of the metals to the opacity vanishes. These very metal-poor stars develop smaller convective cores during central H-burning and subsequently less massive CO cores. Our values of $M_{\rm up}$ range between $7.25 M_\odot$ and $9.25 M_\odot$ and are qualitatively in good agreement with other works (Becker & Iben 1979, 1980, Maeder & Meynet 1989, Ritossa *et al.* 1999) but large differences can arise when extra-mixing is included. For example, Bertelli *et al.* 1985 find a decrease in $M_{\rm up}$ from 9 to $6 M_\odot$ when they allow for some core overshooting. The dependence on metallicity compares relatively well with the results of Bono *et al.* (2000). However in their computations, $M_{\rm up}$ presents a minimum around $Z = 10^{-3}$ compared to $Z = 10^{-4}$ in our models and their values are systematically lower than ours.

7.3 $M_{\rm n}$: *mass transition between NeO white dwarfs and electron capture supernovae*

The fate of the NeO core depends on the competing effects of core growth during the TP-SAGB phase and mass loss. To estimate the impact of mass loss rate on the final evolution, we have used a constant core growth rate $\dot{M}_{\rm core} = 5 \times 10^{-7} M_\odot$ yr^{-1} representative of SAGB stars and considered 2 constant mass loss rates equal to $\dot{M}_1 = 3 \times 10^{-5} M_\odot$ yr^{-1}and $\dot{M}_2 = 10^{-4} M_\odot$ yr^{-1}.

To evaluate $M_{\rm n}$ at a given metallicity, for each stellar models we calculate the remaining NeO core mass when all the envelope has been removed. If this value is less than $M_{\rm EC}$, then we get a NeO white dwarf otherwise a neutron star. The results displayed in Fig. 8 show that, for a given mass loss rate, $M_{\rm n}$ decreases when moving from $Z = 0.04$ to $Z \simeq 10^{-4}$ and then slightly increases at lower metallicity. The reasons are the same as explained before for $M_{\rm up}$ and result from opacity effects. With decreasing Z, stars develop more massive NeO cores at the end of C burning and $M_{\rm EC}$ can be reached more easily. For a given metallicity, an increase in the mass loss rate shifts $M_{\rm n}$ toward higher values. Indeed if $\dot{M}$ increases, the initial NeO core mass must be larger in order to reach the $1.37 M_\odot$ at the end of the TP-SAGB phase. Our values of $M_{\rm n}$ range between ~ 9 and $11 M_\odot$ depending on the parameters and are subject to large uncertainties mainly because of our poor knowledge of $\dot{M}$ in these stars.

7.4 $M_{\rm SN}$: *mass transition between electron-capture and type II supernovae and the second dredge-up connection*

According to Nomoto (1984), if the mass of the NeO core at the end of carbon burning is larger than $M_{\rm EC}$, the evolution of the star proceeds through all nuclear burning stages giving rise to a type II supernovae. As shown in Fig. 8, $M_{\rm SN}$ globally increases with metallicity especially between $10^{-3} \lesssim Z \lesssim Z_\odot$ and its values range between $\sim 10 - 11 M_\odot$.

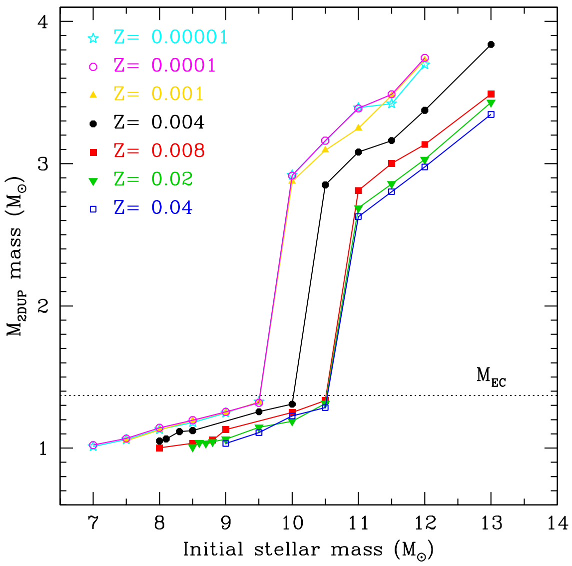

Fig. 9. Mass coordinate of the base of the convective envelope during the second dredge-up $M_{\rm 2DUP}$ as a function of the initial mass for the computed models.

In addition to the critical role played by mass loss, the final course of the evolution of massive SAGB stars is intimately connected to the second dredge-up. For lower mass stars, the 2DUP takes place before C ignition (§4) and contributes to reduce the mass of the H-exhausted core below the Chandrasekhar mass ($M_{\rm Ch}$) thus avoiding core collapse. In more massive stars however, the absence or limitation of such a deep mixing leads to the formation of massive cores ($M_{\rm c} > M_{\rm Ch}$). Figure 9 illustrates the behavior of $M_{\rm 2DUP}$, the minimum mass coordinate of the envelope during the 2DUP, as a function of $M_{\rm ini}$ for the different metallicities covered in this study. The abrupt decrease in $M_{\rm 2DUP}$ between $9.5M_\odot \lesssim M_{\rm ini} \lesssim 10.5M_\odot$ is the direct consequence of the action of the 2DUP in lower mass stars. For solar metallicity models, the discontinuity occurs around $\sim 10.5M_\odot$ and decreases to $\sim 9.5M_\odot$ for metal poor stars. We also note that stars with $M_{\rm 2DUP} > M_{\rm Ch}$ all have a core mass $M_{\rm c} > M_{\rm EC}$ at the end of carbon burning. Consequently, if $M_{\rm 2DUP} > M_{\rm Ch}$ a type II supernovae will ensue.

From Fig. 8, we now have a more general picture of the final evolution of these stars. It is worth noting that the mass range for the formation of electron capture supernovae is extremely narrow (a few $0.1M_\odot$) and may be almost prevented from the evolution of single stars (see Podsiadlowski *et al.* 2004). The mass range for the formation NeO white dwarfs is also confined to a narrow strip of $\sim 1M_\odot$ width and tends to be larger at lower metallicities. On the other hand, the minimum initial mass for a supernovae explosion was smaller in the past as a consequence of the diminishing action of mass loss when the metallicity decreases.

8 Conclusion

The evolution of stars in the mass range $7-12M_{\odot}$ is characterized by the ignition of carbon in region of partial degeneracy. Carbon burning then proceeds in two steps : a violent carbon flash first develops off center and induces a large expansion of the structure which quenches the instability. Core contraction resumes and carbon ignites deeper in the star. However, in this case the degeneracy at the ignition point is weaker and a stable carbon burning flame forms and propagates to the center, converting the CO core into a NeO mixture. Thereafter, if the NeO core mass is less than $\sim 1.37M_{\odot}$, the star enters the SAGB phase. It then undergoes recurrent thermal instabilities of "moderate" amplitude with periods of less that a few hundred years. These thermal pulses are short-lived ($\lesssim$ 1 yr) and hotter than in standard AGB stars and thus may lead to an efficient convective s-process nucleosynthesis. Owing to their larger core mass, the temperature at the base of the envelope of SAGB is also relatively high and HBB is very efficient.

Stars in this mass range can have very different fates which enabled us to determine different mass transitions, depending on nature of the remnant and of the explosion. Although we are confident that the general metallicity dependence of these critical masses is correct, their values are subject to large uncertainties. Among them, the role of mixing at the edge of convective boundaries is of prime importance since it determines the value of the core mass and incidentally the evolution. Our limited knowledge of overshooting, semiconvection, rotationally induced mixing or of the effects of gravity waves represent a large source of uncertainty. The second important parameter is the mass loss rate. What prescription shall we use in this mass range and how does it depend on composition are fundamental questions with no secure answer. This parameter is however crucial in determining the final core mass. In third place, an aspect that has not been touched in this text, concerns the role and influence of a binary companion. Evolution of stars in binary system is much more complicated. This has to do with the mass transfer episodes, with the exchange of angular momentum during the accretion process which modifies the stellar rotation profiles (and the mixing!) or with the effects induced by tidal interactions. Although evolutionary paths leading to the formation of NeO white dwarfs in binary systems have been explored (e.g. Iben & Tutukov 1985, Dominguez *et al.* 1993), many aspects remain to be explored in connection with novae and supernovae explosions.

Massive AGB stars are remarkable objects at the crossroad of different evolutionary paths. Their modeling reveals however challenging for numerical as well as physical reasons. For illustration, the very high resolutions ($\Delta r \lesssim 0.1$ km) needed to correctly follow the propagation of the flame front or the physics relative to the convective URCA process that must be included in the late stages of the evolution of massive NeO cores. These difficulties, plus the prohibitive amount of CPU time required to follow the hundreds of pulses that animate the SAGB phase, have contributed to further study the most simple "standard" low and intermediate-mass AGB stars. However, we may expect that in the coming years, more on the evolution of these stars will be unrevealed.

Manuel was amazed by stars, by how nature could have built such complex and intriguing nuclei factories. In his never ending quest to understand the great details of stellar structure and to break the mysteries of their evolution, he was always looking for the crucial theoretical ingredients that should be implemented in his code. Thanks to his hard labor, to his implication in different collaborations and to his foresight, Manuel, with the help of PhD students including Gwenaëlle Leclair, Ana Palacios, Emmanuel Dufour and myself, developed STAREVOL, a powerful stellar evolution code able to model all kind of stars and, at the moment, the only one to include the full treatment of rotational mixing as described by Jean-Paul Zahn in this book.

Massive AGB stars were Manuel's last topic of research. Aware of the relevance of this forgotten stellar population on important issues related to nucleosynthesis and galactic chemical evolution, but too absorbed by his heavy administrative responsibilities, he was unfortunately not able to involve himself to the extent he desired. Following his idea, massive AGB stars have become the central theme of my research activities. More than a scientific testament, it is the last gift from a friend, a marvelous present that admirably illustrates the complexity and beauty of his beloved stars.

References

Barkat Z., Reiss Y., Rakavy G. 1974, ApJ, 193, L21

Baron E., Cooperstein J., Kahana S. 1987, ApJ, 320, 300

Beaudet G., Salpeter E.E. 1969, ApJ, 155, 203

Becker S.A., Iben I. 1979, ApJ, 232, 831

Becker S.A., Iben I. 1980, ApJ, 237, 111

Bertelli G., Bressan A.G., Chiosi, C. 1985, A&A, 150, 33

Barkat Z., Reiss Y., Rakavy G. 1974, ApJ, 193, L21

Bono G., Caputo F., Cassisi S. *et al.* 2000, ApJ, 543, 955

Boothroyd A.I., Sackmann I.-J. 1998, ApJ, 328, 671

Boozer A.H., Joss P.C., Salpeter E.E. 1973, ApJ, 181, 393

Bressan A., Fagotto F., Bertelli G., Chiosi C. 1993, A&AS, 100, 647

Busso M., Gallino R., Lambert D.L., Travaglio C., Smith V.V. 2001, ApJ, 557, 802

Cameron A.G.W. and Fowler W.A. 1971, ApJ, 164, 111

Cassisi S., Castellani V. 1993, ApJS, 88, 509

Coc A., Vangioni-Flam E., Descouvemont P. *et al.* 2004, ApJ, 600, 544

Denissenkov P.A., Tout C.A. 2003, MNRAS, 340, 722

Dominguez I., Tornambé A., Isern J. 1993, ApJ, 419, 268

Eldridge J.J., Tout C. 2004, Mem. S.A.It., 75, 694

Frost C.A., Lattanzio J.C. 1996, ApJ, 473, 383

Fryer C.L. 1999, ApJ, 522, 413

Gallino R., Arlandini C., Busso M. *et al.* 1998, ApJ, 497, 388

Garcia-Berro E., Iben I. 1994, ApJ, 434, 306
Garcia-Berro E., Ritossa C., Iben I 1997, ApJ, 485, 765
Goriely S., Mowlavi N. 2000, A&A, 362, 599
Goriely S., Siess L. 2004, A&A, 421, L25
Goriely S., Siess L. 2005, IAU symposium 228, in press
Grevesse N., Noels A., Sauval A.J. 1996, ASPC, 99, 117
Gutierrez J., Garcia-Berro E., Iben I. *et al.* 1996, ApJ, 459
Hashimoto M., Iwamoto K., Nomoto K. 1993, ApJ, 414, L105
Herwig F. 2000, A&A, 360, 952
Herwig F., Lugaro M., Langer N. 2003, ApJ, 593, 1056
Hillebrandt W., Wolff R.G., Nomoto K. 1984, A&A, 133, 175
Iben I., Renzini A. 1982, A&A, 263, L23
Iben I., Ritossa C., Garcia-Berro E. 1997, ApJ, 489, 772
Iben I., Tutukov 1985, ApJS, 58, 661
Langer N., Heger A., Wellstein S., Herwig F. 1999, A&A, 346, L37
Maeder A., Meynet G. 1989, A&A, 210, 155
Mayle R., Wilson J.R. 1988, ApJ, 334, 909
Miyaji S., Nomoto K. 1987, ApJ, 318, 307
Miyaji S., Nomoto K., Yokoi K., Sugimoto D. 1980, Pub. Astron. Soc. Japan 32, 303
Nomoto K. 1984, ApJ, 277, 791
Nomoto K. 1987, ApJ, 322, 206
Podsiadlowski P., Langer N., Poelarends A.J.T *et al.* 2004, ApJ, 612, 1044
Pols O.R., Tout C.A 2001, Mem. S.A.It., 72, 299
Rakavy G., Shaviv G., Zinamon Z. 1967, ApJ, 150, 131
Ritossa C., Garcia-Berro E., Iben I. 1996, ApJ, 460, 489
Ritossa C., Garcia-Berro E., Iben I. 1999, ApJ, 515, 381
Schwarzschild M., Harm R.1965, ApJ, 142, 855
Siess L. 2006, A&A, in press
Siess L., Goriely S., Langer N. 2004, A&A, 415, 1089
Siess L., Livio M., Lattanzio J. 2002, ApJ, 579, 329
Siess L., Pumo M.L. 2006, A&A, in preparation
Straniero O., Dominguez I., Imbriani G., Piersanti L. 2003, ApJ, 583, 878
Straniero O., Chieffi A., Limongi M. *et al.* 1997, ApJ, 478, 332
Timmes F.X., Woosley S.E., Taam R.E. 1994, ApJ, 420, 348
Van Eck S., Goriely S., Jorissen A., Plez B. 2001, Nature 412, 793
Vassiliadis E., Wood P.R. 1993, ApJ, 413, 641
Wanajo S., Tamamura M., Itoh N. *et al.* 2003, ApJ, 593, 968
Wheeler J.C., Cowan J.J., Hillebrandt W. 1998, ApJ, 493, L101
Wood P.R. 1981, ApJ, 248, 311
Yoon S.C., Langer N., van der Sluys M. 2004, A&A, 425, 207